

Overall Temporal Synchrotron Emissions from Relativistic Jets: A Diabatic and Radiative Breaks

Zhuo Li[?], Z. G. Dai^Y and T. Lu^Z

Department of Astronomy, Nanjing University, Nanjing 210093, China

(submitted to MNRAS)

ABSTRACT

We discuss the afterglow emission from a relativistic jet that is initially in the radiative regime in which the accelerated electrons are fast cooling. We note that such a “synchrotronic” jet decelerates faster than an adiabatic jet does. We also take into account the effect of strong inverse-Compton scattering on the cooling frequency in the synchrotron component and therefore on the light curve decay index. We find that there are two kinds of light-curve break for the jet effect. The first is an “adiabatic break” if the electrons become slow cooling before the jet enters a spreading phase, and the second is a “radiative break” which appears on the contrary case. We then show how a relativistic jet evolves dynamically and derive the overall temporal synchrotron emission in both cases, focusing on the change in light curve decay index around the break time. Finally, in view of our results, we rule out two cases for relativistic jets to account for the observed light curve breaks in a few afterglows: (i) an adiabatic jet with strong Compton cooling ($\gamma > 1$) and with the cooling frequency ν_c locating in the observed energy range; (ii) a radiative jet with a significant fraction of total energy occupied by electrons ($\epsilon_e \ll 1$).

Key words: gamma rays: bursts | radiation mechanisms: non-thermal

[?] lizhuo@nju.edu.cn

^Y daizigao@public1.ptt.js.cn

^Z tlu@nju.edu.cn

1 INTRODUCTION

It is widely believed that gamma-ray bursts (GRBs) and their afterglows are caused by the dissipation of kinetic energy of an ultrarelativistic ejecta, with Lorentz factor $\gamma > 100$, releasing from the central engine (so-called "reball" model, see Piran 1999 and van Paradijs, Kouveliotou & Wijers 2000 for detailed reviews). GRBs are the most energetic explosive phenomena in astronomy. In the reball model, the collisions among different shells within the ejecta might be expected to produce a prompt burst (Paczynski & Xu 1994; Rees & Meszaros 1994), and subsequently the ejecta interacts with its surrounding medium, producing a long-term and broad-band afterglow (Paczynski & Rhoads 1993; Meszaros & Rees 1997). In the standard afterglow picture, the ejecta drives a relativistic blast wave expanding into the surrounding medium, which approaches a self-similar solution (Blandford & McKee 1976) after a short time once the swept-up medium attains an energy comparable to the initial energy of the burst. Electrons in the cold medium are heated in the shock front to highly relativistic energy and produce a broad-band afterglow via synchrotron/inverse-Compton emission. The predicted emission spectrum and light curve (Meszaros & Rees 1997; Sari et al. 1998) have met essential successes in describing the behavior of afterglows (e.g., Vietri 1997; Waxman 1997a,b; Wijers et al. 1997). The recent observations on GRB afterglows have lead to numerous numerical calculations to model the observed afterglows (e.g., Huang et al. 2000a,b; Gou et al. 2001; Panaitescu & Kumar 2001; Panaitescu 2001).

We re-investigate the dynamical evolution and temporal emission of afterglows by considering three aspects. (i) The electrons heated by the shock are always fast cooling when the cooling timescale for these electrons is shorter than the dynamical timescale (see, e.g., Waxman 1997a; Meszaros et al. 1997; Sari et al. 1998), and the afterglow evolution should be in the radiative regime rather than the adiabatic one as long as a significant fraction (ϵ_e) of the reball energy is transferred to newly heated electrons, $\epsilon_e \ll 1$. This shock decelerates faster than an adiabatic shock, as pointed out by Bottcher & Dermer (2000). The newly launched HETE-2 satellite, due to its rapid and accurate location of GRBs, should lead to much more follow-up observations on early X-ray and optical emission, allowing a detailed analysis of the afterglow feature. (ii) The inverse-Compton emission is important in afterglows (Panaitescu & Meszaros 1998; Wei & Lu 1998; Totani 1998; Chiang & Dermer 1999; Dermer, Bottcher & Chiang 2000; Panaitescu & Kumar 2000; Sari & Esin 2001; Zhang &

Mészáros 2001). When the inverse-Compton cooling of electrons dominates the synchrotron cooling, the temporal synchrotron emission is influenced by changing the scaling law of the cooling frequency ν_c (defined later) with time. (iii) Jets are especially important in GRBs since they are relevant to almost all aspects of GRB phenomenon, e.g. the total energy released in a GRB, the burst rate, the ejection mechanism of the central engine and the dynamical evolution of the ejecta. It is of particular interest that the light curves of afterglows might be changed when the jet enters a spreading phase, as pointed out by Rhoads (1999), Sari et al. (1999) and Dai, Huang & Lu (2001). The discovery of polarization in the afterglow of GRB 990510 has shown evidence for a jet-like outflow (Covino et al. 1999; Wijers et al. 1999).

We consider GRBs as jets. The jet evolves as spherical-like expansion before entering the spreading phase (Rhoads 1999; Sari et al. 1999), and the heated electrons are always fast cooling at first. This radiative and spherical-like phase ends once either (1) the electrons become slow cooling or (2) the relativistic jet transits to the spreading phase. So a "radiative break" in the light curve may appear for the case where the jet transits to the spreading phase when the electrons are still fast cooling and the jet is in the radiative regime. This break is different from the widely discussed "adiabatic break" for the case where the transition occurs in the adiabatic regime in which the electrons have been slow cooling. In this work we derive the overall analytical evolution of synchrotron emission from a relativistic jet. We first introduce the dynamical evolution of a relativistic jet in section 2. Then the temporal evolution of synchrotron emission from the jet is calculated in section 3. In section 3.1 we analyze the radiative regime when the jet evolution is spherical-like. Section 3.2 discusses the adiabatic break in which the electrons become slow cooling before the jet evolves into the spreading phase while section 3.3 explores the radiative break in which the transition to the spreading phase occurs in the radiative regime. We give some discussions and conclusions in section 4.

2 DYNAMICAL EVOLUTION OF RELATIVISTIC JETS

Let's consider a relativistic jet expanding into its surrounding medium with an initial half opening angle of θ_0 , a laterally-spreading velocity of c_s and a bulk Lorentz factor of Γ . Though the shock is beamed, the jet evolution is spherical-like as long as $\Gamma > \theta_0^{-1} (c_s = c)$.

Because the electrons accelerated by a shock are always fast cooling at first, the jet should be radiative if the energy density of the electrons is a significant fraction ϵ_e of the total energy density of the shocked medium. The jet hydrodynamics in this radiative regime will be different from the well known self-similar solution for adiabatic blast waves derived by Blandford & McKee (1976), $\dot{M} / r^{3/2}$, where r is the shock radius. Thus, the jet behaves as a radiative and spherical-like expansion at the initial stage. The jet evolution later is divided into two cases. (a) In the case of an adiabatic break, the accelerated electrons become slow cooling before the jet evolves into a spreading phase, so the jet exhibits an adiabatic and spherical-like evolution as $\dot{M} / r^{3/2}$ sequentially and finally a spreading phase of dropping exponentially with increasing r . (b) In the case of a radiative break, the jet transition into the spreading phase occurs in the radiative regime where the shocked electrons are still fast cooling, and therefore the jet evolves from the initial radiative spherical-like phase to the spreading phase directly, without the second phase of adiabatic and spherical-like evolution of case (a). Fig. 1 depicts these two cases of the dynamical evolutions of relativistic jets.

Since the evolution of an adiabatic spherical blast wave is well known, we introduce here only the dynamics of so-called "semi-radiative" blast waves for the initial stage of radiative and spherical-like evolution and of the radiative jet for the final stage in the case of a radiative break.

Recently, for semi-radiative blast waves, in which the energy radiated is considerable to affect the evolution of the blast waves, Cohen et al. (1998) have also derived a self-similar solution under the assumption that a fixed fraction of the energy generated by the shock is radiated away. This assumption is applicable at early times, since the heated electrons are in the fast-cooling regime and a fixed fraction of the total energy that has been transferred to electrons is radiated away while the protons do not radiate their energy and remain hot. Following Cohen et al. (1998), the radius r and the Lorentz factor γ of a semi-radiative blast wave are in relation of γ^2 / r^m , and they evolve with the observer time as

$$r = r_0 \frac{t}{t_0}^{\frac{1}{m+1}}; \quad (1)$$

$$\gamma = \gamma_0 \frac{t}{t_0}^{\frac{m}{2(m+1)}}; \quad (2)$$

$$m = \frac{(1 + \gamma^2) + 3(1 + \gamma^2)(4 - k)}{3}; \quad (3)$$

Here γ_0 is the initial coasting Lorentz factor of the jet, r_0 is the deceleration radius where the energy in the shocked medium equals that in the original explosion, t_0 is the observer time at which the deceleration radius is reached, ϵ is a fraction of energy that is radiated away and should be understood as $\epsilon = \epsilon_e$ in the fast cooling regime, and k parameterizes the proton number density n of the surrounding medium with $n = A r^{-k}$. For $k = 0$ and $\epsilon = (0|1)$, m varies from 3 to 12 and the Lorentz factor of the blast wave evolves based on r/t^{3-8} to r/t^{6-13} . It is the adiabatic solution case with $\epsilon = 0$. Denoting the energy in the original explosion as E_0 , and the redshift of this explosion as z , we have

$$r_0 = \frac{3-k}{4A} \frac{E_0}{m_p c^2}^{\frac{1}{3-k}}; \quad (4)$$

$$t_0 = \frac{r_0(1+z)}{2\gamma_0 c}; \quad (5)$$

In the fully radiative ($\epsilon = 1$) case, the scaling r/t^6 differs from the widely used Blandford-McKee solution, r/t^3 (see, e.g., Sari, Piran & Narayan 1998, Bottcher & Dermer 2000), which assumes a thin shell with a cooled interior and the kinetic energy of the shell can be written as $E_k = (\gamma - 1)M\gamma$, where M is the shell mass. In fact, the quantities, such as velocity, density and energy density, should be a function of distance from the shock front. Thus, we prefer to use the self-similar solution of Cohen et al. (1998) which assumes a shell with finite width within which the interior exerting a pressure onto the outer. Hereafter we use the equations above to describe the evolution of blast waves in the following calculations.

For the dynamics of a relativistic jet, Rhoads (1999) has derived an adiabatic solution, in which the jet evolution in the spreading phase is an exponential slowing down of γ with increasing r . We can expect the jet slows down even faster if it is in the radiative regime and loses energy more quickly than an adiabatic jet does. Thus, for a radiative jet, r is practically a constant during the spreading phase. Therefore, from $r/t^2 \sim ct$, we have the same scaling relation of r/t^{1-2} as that of an adiabatic jet.

3 TEMPORAL EVOLUTION OF SYNCHROTRON EMISSION SPECTRA

As shown later, the previous studies on jetted afterglows are only suitable for the adiabatic break case with weak Compton-cooling effect. At first, we concentrate on deriving the spectra

and light curves in the initial radiative and spherical-like stage, and then we discuss the light-curve change around the break time in both the adiabatic and radiative break cases with strong or weak Compton-cooling effect.

3.1 Radiative and spherical-like phases

We only consider the emission from the accelerated electrons, neglecting the emission from the hot protons. The electron distribution is assumed to be a power-law of Lorentz factor, $N(\gamma_e)/\gamma_e^p$, with the minimum random Lorentz factor,

$$\gamma_m = \frac{2}{(1+X)} \frac{(p-2)m_p}{(p-1)m_e} \beta_e; \quad (6)$$

where X is the usual hydrogen mass fraction of the surrounding medium. We assume that $p > 2$ here after so that the total electron energy is dominated by electrons with γ_m . Recently Dai & Cheng (2001) have studied the case of $1 < p < 2$. The strength of the magnetic field in the co-moving frame is given by

$$B^0 = \frac{q}{c} \frac{1}{32} n m_p \beta_e; \quad (7)$$

where β_e is a fraction of the total internal energy density that is carried by the magnetic field.

We concentrate here on the radiative regime when the cooling timescale for electron with γ_m is shorter than the dynamical timescale, $t = \frac{1+z}{c} R \frac{dr}{dr} = \frac{2(1+z)}{2+m} \frac{r}{c}$ for $r \propto \gamma_m^{-2}$. In this case, the distribution of electrons extends to a lower Lorentz factor γ_c as a power-law γ_e^{-2} for $\gamma_c < \gamma_e < \gamma_m$ and $\gamma_e^{-(p+1)}$ for $\gamma_e > \gamma_m$, where γ_c is the Lorentz factor of electrons that cool on the dynamical timescale t ,

$$\gamma_c = \frac{3 m_e c^2 (2+m)}{T (1+Y) B^0 r}; \quad (8)$$

Here we have considered the inverse-Compton cooling of electrons by the Compton parameter (Sari & Esin 2000)

$$Y = \frac{1}{2} + \frac{1}{2} \frac{1}{1 + 4 \frac{\gamma_e}{\gamma_B}}, \quad \begin{cases} \geq \frac{\gamma_e}{\gamma_B}; & \text{if } \frac{\gamma_e}{\gamma_B} \leq 1; \\ \geq \frac{\gamma_B}{\gamma_e}; & \text{if } \frac{\gamma_e}{\gamma_B} > 1; \end{cases} \quad (9)$$

where γ_B is a fraction of the electron energy that is radiated away. We should note that $\gamma_B = 1$ for fast cooling and $\gamma_B = (\gamma_c/\gamma_m)^{2-p}$ for slow cooling.

The simple model of synchrotron spectra of afterglows is a broken power-law with three break frequencies. One is the absorption frequency ν_a below which the synchrotron photons

are self-absorbed by electrons. The other two are the characteristic synchrotron frequencies according to electrons with Lorentz factor γ_m and γ_c , denoted ν_m and ν_c , respectively. Following the improved treatment of synchrotron emission by Wijers & Galametz (1999), we have

$$\nu_m = \frac{x_p e}{m_e c (1+z)} B^0 \nu_m^2; \quad (10)$$

$$\nu_c = \frac{0.286 e}{m_e c (1+z)} B^0 \nu_c^2; \quad (11)$$

where the dimensionless factor $x_p = 0.64$, for $p = 2$.

The absorption frequency is defined to be the point where $\tau = 1$. Note that in the co-moving frame of the shocked shell (denoted with a prime), the absorption coefficient κ_0 scales as $\kappa_0 / \nu_0^{(p+4)/2} = \text{const}$ for $\nu_0 > \nu_p^0$ in $(\nu_m^0; \nu_c^0)$ and $\kappa_0 / \nu_0^{5/2} = \text{const}$ for $\nu_0 < \nu_p^0$ (Waxman 1997b), where ν_p^0 is the index of the distribution of those electrons relevant to synchrotron self-absorption around ν_0 . For the absorption coefficient at co-moving cooling frequency

$$\kappa_c^0 = \frac{3(1+z)}{8} \frac{e^3}{m_e} \frac{1}{2 m_e^2 c^3} C B^0 \nu_c^0{}^3 \quad (4) \quad (12)$$

where $C = 2(1+X)n_e$ (coming from $R_m C_e^2 d_e = \frac{1+X}{2} 4\pi n$ for $\nu_m < \nu_c$), $\nu_0^0 = (\sin \theta)^2 \sin \theta$ and $\Gamma(y)$ is the Gamma function. The optical depth at ν_c^0 is then $\tau_c = \kappa_c^0 r^0$, where $r^0 = r/4$ is the co-moving width of the shocked shell, thus we can get the absorption frequency

$$\nu_a = \nu_c^0{}^{3/5} = \nu_c^0 \frac{r^0{}^{3/5}}{4} \quad (13)$$

for $\nu_a < \nu_c$ in the radiative regime. We have neglected the case of $\nu_a > \nu_c$ since $\nu_c > 1$ lasts for only few seconds in general parameter space.

The peak flux in the synchrotron spectrum is

$$F_m = \frac{p \bar{3} p e^3}{4 d_1^2 (1+z) m_e c^2} B^0 N_e; \quad (14)$$

where p is a factor defined by Wijers & Galametz (1999), which is $p = 0.64$ for $p = 2$ here, d_1 is the luminosity distance, and N_e is the number of electrons in the shocked shell and given by

$$N_e = \frac{2(1+X)}{3-k} A r^3 k; \quad (15)$$

Substituting γ and r with aid of equations (1)–(3), one obtains expressions of ν_m , ν_c , ν_a and F_m (shown in Appendix), and their scaling relations with the observer's time are

$$\nu_m / t^{\frac{k+4m}{2(1+m)}}; \quad (16)$$

$$\nu_c / t^{\frac{4-3k}{2(1+m)}}; \quad (17)$$

$$\nu_a / t^{\frac{9k+6m-8}{5(1+m)}}; \quad (18)$$

$$F_m / t^{\frac{3k+2m-6}{2(1+m)}}; \quad (19)$$

Given these three break frequency and peak flux, we can calculate the synchrotron spectrum and light curve. Note that $\nu_a < \nu_c < \nu_m$ in the radiative regime. For a homogeneous medium, $k = 0$ (Note that hereafter in this paper the discussions are all concerned about this homogeneous medium case), the fluxes in the four frequency ranges divided by three break frequencies evolve as

$$\begin{aligned} F_{<\nu_a} &= F_m \frac{\nu_m^2}{\nu_a^2} \frac{\nu_c^{1-3}}{\nu_m^{1-3}} / t^2; \\ F_{\nu_a < \nu_c} &= F_m \frac{\nu_m^{1-3}}{\nu_c^{1-3}} / t^{\frac{3m-11}{3(1+m)}}; \\ F_{\nu_c < \nu_m} &= F_m \frac{\nu_m^{1-2}}{\nu_c^{1-2}} / t^{\frac{m-2}{1+m}}; \\ F_{>\nu_m} &= F_m \frac{\nu_m^{p-2}}{\nu_m^{p-2}} \frac{\nu_c^{1-2}}{\nu_c^{1-2}} / t^{\frac{mp-2}{1+m}}; \end{aligned} \quad (20)$$

The light curve decay indexes are relevant to β ($= \beta_e$), and shown in Fig. 2. Therefore, observations of early-time afterglows following a prompt burst can help to determine the parameter β_e .

We have neglected the effect of inverse-Compton process on the shape of synchrotron spectrum, because the Thomson optical depth of synchrotron photons is generally very small and only a negligibly small fraction of synchrotron photons is scattered. Besides, the typical energy of inverse-Compton emission, $\nu_m^{IC} = \gamma^2 \nu_m$, usually far exceeds that of the synchrotron component which we are concerned about, since the accelerated electrons are always relativistic because $\gamma_m \gg 1$ for relativistic blast waves.

The end of this radiative and spherical-like stage is determined by the minimum of two time scales. One is the time t_{cm} when $\nu_m = \nu_c$. After this time, the accelerated electrons around ν_m become slow cooling so that the shock is practically not radiative any more and transits from the radiative to the adiabatic phase (The transition is gradual due to the gradual change of β from β_e to 0, since $\beta = \beta_e$). Thus, in this transition phase, the blast wave evolution will not be self-similar). Another is the break time t_{jet} when $\gamma_0^{-1}(c_s=c)$

and the jet enters the spreading phase. Having the expressions of \dot{m} and \dot{c} we can derive t_{cm} (a detailed expression given in Appendix). With the aid of the evolution of \dot{c} , we have the break time

$$t_{\text{jet}} = t_0 \left(\frac{\dot{c}_0}{\dot{c}} \right)^{\frac{2(m+1)}{m}} \quad (21)$$

(see a detail in Appendix). Here we have taken $\dot{c}_s = \dot{c}$. Fig. 3 shows two times, t_{cm} and t_{jet} , varying with \dot{c}_e . It is the adiabatic break case in the small \dot{c}_e end since $t_{\text{cm}} < t_{\text{jet}}$, while the radiative break case tends to appear in the right end where $t_{\text{cm}} > t_{\text{jet}}$.

3.2 A diabatic jet break

3.2.1 Adiabatic and spherical-like phase

We first discuss the case of $t_{\text{cm}} < t_{\text{jet}}$, which corresponds to Fig. 1a. When the time t_{cm} is reached, the jet enters an adiabatic and spherical-like stage which have been studied by many authors. The blast wave evolves as $\dot{c} \propto r^{-3/2} \propto t^{-3/8}$. We have the well-known scaling relations

$$\dot{m} \propto t^{-3/2}; \quad \dot{c} \propto t^{-1/2} \quad (Y < 1); \quad \dot{a} \propto t^0; \quad F_m \propto t^0: \quad (22)$$

In some B cases, i.e. a magnetic field extremely far below equipartition like the cases of GRB 971214 (Wijers & Galametz 1999) and 990123 (Galametz et al. 1999), the adiabatic blast wave will be strong Compton cooling with $Y \ll 1$. The evolution of the cooling frequency \dot{c} becomes somewhat complicated if the $Y > 1$ case is considered. We combine $Y \propto \dot{P}^{-1} \propto (\dot{c} \dot{m})^{(2-p)/2}$ and $\dot{c} \propto (Y B^0 r)$ for $Y > 1$ with $\dot{c} \propto B^0 \dot{c}^2$ to obtain the general scaling

$$\dot{c} \propto t^{-2-2p/(4-p)} \quad (Y > 1): \quad (23)$$

For an adiabatic and spherical-like jet, this becomes

$$\dot{c} \propto t^{-3+2/(4-p)} \quad (Y > 1): \quad (24)$$

We can see that \dot{c} might increase or decrease with time, depending on whether $p > 8/3$ or $p < 8/3$, respectively. Note that Y is also a function of time due to decreasing \dot{c} . So if $\dot{c}_e \ll B$, then $Y > 1$ in the beginning fast cooling phase, and $Y \propto (r^2)^{\frac{p-2}{4-p}}$ generally in the slow cooling phase. The slowing-down leads to $Y \propto t^{\frac{1}{2}(\frac{p-2}{4-p})}$ for $\dot{c} \propto t^{-3/8}$, or $Y \propto t^{\frac{p-2}{4-p}}$ for $\dot{c} \propto t^{-1/2}$ until $Y \ll 1$ (We assume $p < 4$ here after, which is consistent with the observations

which show that all afterglows appear to have the electron energy distribution of $p < 4$. Thus there might be a transition from the strong Compton cooling ($Y > 1$) to the weak Compton cooling ($Y < 1$) phase, as pointed out by Sari et al. (2000). However, if ϵ_B , then $Y < 1$ throughout.

It is now easy to derive the light curves in four frequency ranges

$$\begin{aligned}
 F_{< \nu_a} &= F_m \frac{\nu_a^2}{\nu_m^2} \frac{\nu_m^{1=3}}{\nu_a^{1=3}} / t^{1=2}; \\
 F_{\nu_a < \nu_m} &= F_m \frac{\nu_m^{1=3}}{\nu_m^{1=3}} / t^{1=2}; \\
 F_{\nu_m < \nu_c} &= F_m \frac{\nu_m^{(p-1)=2}}{\nu_m^{(p-1)=2}} / t^{3(p-1)=4}; \\
 F_{> \nu_c} &= F_m \frac{\nu_c^{p=2}}{\nu_m^{p=2}} \frac{\nu_m^{(p-1)=2}}{\nu_c^{(p-1)=2}} \begin{cases} \geq \nu_c^{p=2} t^{3p=4+1=(4-p)} & (Y > 1); \\ \leq \nu_c^{p=2} t^{3p=4+1=2} & (Y < 1); \end{cases}
 \end{aligned} \tag{25}$$

Note that the transition of a jet from the radiative phase to the adiabatic phase at t_{cm} results in a flattening of the light curve in the energy range of $> \nu_c$, and even the light curve is more flattening in the case of $Y > 1$ than in the case of $Y < 1$.

3.2.2 Spreading phase

A break time is reached when $\gamma_0^{-1}(c_s=c)$. In this adiabatic break case, Eq. (21) is invalid to calculate this break time since an adiabatic and spherical-like phase has appeared before the final spreading phase. We need to derive the break time again as follows. From the integral $t_{jet}^a - t_{cm} = \frac{R_{jet}}{r_{cm}} \frac{dr}{2\gamma^2 c}$ where $r_{jet} = (\gamma_{cm} - 1)^{2=3} r_{cm}$, the break time is given by

$$t_{jet}^a \sim \frac{1+m}{4} (\gamma_{cm} - 1)^{8=3} t_{cm} \tag{26}$$

(see a detail in Appendix) for $t_{jet}^a - t_{cm}$ or $\gamma_{cm} - 1$. This value is larger than that of Eq. (21).

Having entered the spreading phase, the jet evolves as $\gamma \propto t^{-1=2}$ and the shock radius r can be regarded as a constant. We rewrite the scalings of the break frequencies and the peak flux as

$$\begin{aligned}
 \nu_m &\propto t^{-2}; \quad \nu_c \propto \begin{cases} \geq t^{-2+4=(4-p)} & (Y > 1) \\ \leq t^0 & (Y < 1) \end{cases}; \quad \nu_a \propto t^{-1=5}; \quad F_m \propto t^{-1};
 \end{aligned} \tag{27}$$

It is a rather remarkable result that ν_c is actually increasing with time in the $Y > 1$ case. Therefore the flux turns to evolve as

	spectral index (F / t)	light curve index sphere	(F / t) jet
$m < c$	$(p-1)=2$	$= 3(p-1)=4$ $= 3-2$	$= p$ $= 2+1$
$> c, Y < 1$	$p=2$	$= 3p=4$ $1=2$ $= 3-2$ $1=2$	$= p$ $= 2$
$> c, Y > 1$	$p=2$	$= 3p=4$ $1=(4-p)$ $= 3-2$ $1=(4-2)$	$= p$ $2=(4-p)$ $= 2$ $1=(2)$

Table 1. The spectral index and the light curve index as function of p in the case of an adiabatic jet break. The parameter-free relation between and is given for each case by eliminating p .

$$\begin{aligned}
 F &< a / t^0; \\
 F &_{a < m} / t^{1=3}; \\
 F &_{m < c} / t^{(p-1)=2} p; \\
 F &_{> c} / t^{p+2=(4-p)} (Y > 1); \\
 F &_{> c} / t^{p=2} p (Y < 1);
 \end{aligned} \tag{28}$$

Note that if $Y < 1$, the transition of a relativistic jet into the spreading phase results in a steepening of the light curve in $> m$, with decay index p independent of whether $> c$ or $< c$. But in the case of strong Compton cooling, $Y > 1$, something different happens: the transition yields the same steepening of the light curve into t^{-p} in $m < c$, but due to the cooling frequency c increasing in time, a flattening from $t^{-3p+4-1=(4-p)}$ to $t^{-p+2=(4-p)}$ appears in $> c$. Define the light curve index and the spectral index as $F(t) / t$. Table 1 summarizes the relations between and above m for different cases. Fig. 4 presents the effect of strong Compton cooling on the relation above c .

3.3 Radiative jet break

If $t_{\text{jet}} < t_{\text{cm}}$, corresponding to Fig. 1b, the break time is first reached to end the spherical-like evolution even when the electrons are still fast cooling and the jet might be in the radiative regime with $\epsilon_e = 1$. In the spreading phase the effect of sideways expansion dominates the jet evolution, then the dynamics is $\propto t^{-1=2}$. And the electrons turn from fast cooling into slow cooling in the spreading phase.

3.3.1 Fast cooling

With the same jet evolution as that in the spreading phase of an adiabatic jet, $r / t^{1=2}$, we have the same scalings of γ_m , γ_c and F_m ,

$$\gamma_m / t^{-2}; \gamma_c / t^0; F_m / t^{-1}. \quad (29)$$

Since $\beta = 1$ for fast cooling, the Compton parameter Y is then a constant and the scaling relation of γ_c with observer's time is the same as in the case of $Y = 1$. Next we derive the remaining absorption frequency ν_a . In this case of fast cooling, the electrons responsible for low energy emission are those with γ_c , and therefore $\nu_a = \gamma_c^3 \nu_c^{3=5}$. In the co-moving frame of the shocked medium, the absorption coefficient at cooling frequency is given by Eq. (12),

$$\kappa_0 / C B^2 \gamma_c^3 / r^{5=5}, \text{ and the optical depth at cooling frequency is } \tau_c / \gamma_c^0 r = \tau / r^{6=4}.$$

Thus, we have

$$\nu_a / r^{8=5-12=5} / t^{-6=5}. \quad (30)$$

With the scalings above, the spectra in fast cooling phase, where $\nu_a < \nu_c < \nu_m$, evolve as

$$\begin{aligned} F_{< \nu_a} &/ t^{-2}; \\ F_{\nu_a < \nu_c} &/ t^{-1=3} t^{-1}; \\ F_{\nu_c < \nu_m} &/ t^{-1=2} t^{-1}; \\ F_{> \nu_m} &/ t^{-p=2} t^{-p}. \end{aligned} \quad (31)$$

When the energy of accelerated electrons are nearly in equipartition with protons, we have $\beta = 1$, where the jet evolution in the fully-radiative and spherical-like phase, $r / t^{6=13}$, is closer to that of the spreading phase, $r / t^{1=2}$. So we can expect that the light-curve break due to sideways expansion is less obvious. In fact, if $\beta = 0.6$, which is the estimated value for GRB 970508 by Granot et al. (1999), and $p = 2.4$, the steepening around the break time from $t^{-1.9}$ to $t^{-2.4}$ is really weak. Furthermore, the numerical calculations of jetted afterglows by some authors (e.g., Moderski et al. 1999; Wei & Lu 2000; Huang et al. 2000a,b) showed a smooth change in light curves, and thus we expect that there may be no light curve breaks observed in the case discussed here. That is to say, no break doesn't mean a burst without beaming. Table 2 summarizes the relation above ν_m before and after the break time t_{jet} . Fig. 5 depicts further the relation above ν_c .

spectral index (F_ν / ν)		light curve index sphere	(F_ν / t) jet
$\alpha_c < \alpha_m$	$p=2$	$= (m-2)/(1+m)$ $= 1/4 \quad \quad 10/13$	$= 1$
$\alpha_c > \alpha_m$	$p=2$	$= (m-2)/(1+m)$ $= (3-1)/2 = 1 \quad \quad (24-2)/13 = 2$	$= p$ $= 2$

Table 2. Same as Table 1 but in the case of a radiative jet break. Note that $m = 3 \frac{1}{2}$ has been used to yield the range of α .

3.3.2 Slow cooling

Finally, when $\alpha_m = \alpha_c$, the electrons become slow cooling, the temporal scalings of the break frequencies and the fluxes are the same as those in the later spreading phase of an adiabatic jet in section 3.2.2. So Eq. (28) are valid here. But the t_{cm} calculated in section 3.2.2 is not valid here because the jet has been in the spreading phase rather than the spherical-like phase. This time becomes

$$t_{\text{cm}}^r = t_{\text{jet}} \frac{m_{\text{jet}}}{c_{\text{jet}}} \quad (32)$$

(see a detail in Appendix), where the subscript "jet" denotes the quantities in time t_{jet} .

4 SUMMARY AND DISCUSSION

We have analyzed the whole process of a relativistic jet expanding into a homogeneous environment, from the radiative to adiabatic regime and from the spherical-like to spreading phase. Then we have found two different kinds of light-curve break for the jet effect. One is an adiabatic jet break which appears if the transition of the jet into the spreading phase happens in the adiabatic regime when the accelerated electrons are already slow cooling. This case is widely discussed already. Another is a radiative jet break which corresponds to the jet spreading obviously in the radiative regime when the accelerated electrons are still fast cooling. This case leads to a weaker break in the light curve if $\alpha_e > 1$.

Based on the dynamics, we have derived the light curves of synchrotron emission from jetted afterglows, and summarized our main results as follows. First, in the earliest radiative and spherical-like phase, the light curve decay index is steep and relevant to α_e shown in Eq. (20), e.g., the flux at high energy $\nu > \nu_m$ decays as fast as t^{-2} for $\alpha_e > 1$ and $p > 2/3$. Thus, as pointed out by Bottcher & Dermer (2000), the rapid detections of afterglows at

early times will provide a way to determine the electron energy fraction ϵ_e of total energy density.

Second, if the Compton cooling of electrons dominates the synchrotron cooling, the afterglows will exhibit quite different behaviors from the previous predictions. In the case of an adiabatic jet break, the sharp steepening of light curve in both $< \nu_c$ and $> \nu_c$ is only expected for the case of $\epsilon_e = \epsilon_B = 1$, i.e. $Y < 1$ in the beginning. While for the case of $\epsilon_e = \epsilon_B < 1$, the jet begins with strong Compton scattering ($Y > 1$), and it might dominate total cooling over the whole relativistic stage (Sari & Esin 2000). In this case, the light curve steepening in $< \nu_c$ is accompanied with a flattening (or even a climb) in $> \nu_c$, due to the increasing cooling frequency ν_c for $Y > 1$.

Finally, in the case of a radiative jet break, the late-time change of the dynamical evolution due to jet effect is weaker than in the case of an adiabatic jet break, which results in a weaker light curve break. If $\epsilon_e < 1$, the change is practically smooth, yielding a smooth "break". Thus, this kind of jet will show a singly steep light curve without obvious steepening break in $> \nu_c$, even though the jet is highly collimated with a small θ_0 .

A few GRB afterglows are observed to have an achromatic light curve break, e.g., GRB 990123 (Kulkarni et al. 1999; Castro-Tirado et al. 1999; Fruchter et al. 1999), GRB 990510 (Harrison et al. 1999; Stanek et al. 1999), GRB 991216 (Halpern et al. 2000), GRB 000301C (Rhoads & Fruchter 2001; Masetti et al. 2000; Jensen et al. 2001; Berger et al. 2000; Sagar et al. 2000), GRB 000418 (Berger et al. 2001), and GRB 000926 (Priebe et al. 2001; Harrison et al. 2001; Sagar et al. 2001a; Piro et al. 2001), GRB 010222 (Masetti et al. 2001; Stanek et al. 2001; Sagar et al. 2001b; Cowiik et al. 2001; In 't Zand et al. 2001). Jets in GRBs are usually proposed to account for these breaks. However, in view of our work, two cases of relativistic jets are ruled out to explain these breaks: (i) an adiabatic jet ($t_{\text{cm}} < t_{\text{jet}}$) with strong Compton cooling ($Y > 1$) and the cooling frequency ν_c locating in the observed energy range; (ii) a radiative jet ($t_{\text{cm}} > t_{\text{jet}}$) with a significant fraction of the total energy occupied by electrons ($\epsilon_e < 1$).

It should be noted that all the discussions here are concerned about the relativistic stage. If a relativistic jet expands into a medium as dense as $10^3 - 10^6 \text{ cm}^{-3}$, such as a circumstellar cloud (Galamaz & Wijers 2001), the blast wave must enter the non-relativistic stage within a few days, leading to a steepening of the afterglow light curve (Dai & Lu 1999, 2000).

This transition from the relativistic to non-relativistic stage produces another promising explanation for the broken afterglow light curves.

ACKNOWLEDGMENTS

Z. Li would like to thank D. M. Wei, X. Y. Wang and Y. F. Huang for valuable discussions. The authors thank the anonymous referee for valuable and detailed comments. This work was supported by the National Natural Science Foundation of China under grants 19973003 and 19825109, and the National 973 project (NKBRSG 19990754).

APPENDIX

The time-evolution of the three break frequencies and peak flux in the earliest radiative and spherical-like phase are given below:

$$f_m = f(k; m) \frac{p}{p_1} \frac{2^{1/2}}{(1+X)^2 (1+z)^{1+\frac{k-4}{2(1+m)}}} x_p A^{\frac{k+m-3}{2(k-3)(1+m)}} E_0^{\frac{(k-4)m}{2(k-3)(1+m)}} E_0^{\frac{(k-4)(k+m-3)}{(k-3)(1+m)}} \quad (33)$$

$$\frac{1=2}{B} t_e^{\frac{k+4m}{2(1+m)}} H z;$$

where

$$f_m(k; m) = 2.88 \cdot 10^{13} \cdot 53.32^{\frac{(k-4)m}{(k-3)(1+m)}} (6.00 \cdot 10^{10})^{\frac{k+4m}{2(1+m)}} (3-k)^{\frac{(k-4)m}{2(k-3)(1+m)}}; \quad (34)$$

$$c = f(k; m) (1+Y)^2 (1+z)^{\frac{2-3k-2m}{2(1+m)}} A^{\frac{9-3k+5m}{2(k-3)(1+m)}} E_0^{\frac{(4-3k)m}{2(k-3)(1+m)}} E_0^{\frac{(3k-4)(k+m-3)}{(k-3)(1+m)}} \frac{3=2}{B} t_e^{\frac{4-3k}{2(1+m)}} H z; \quad (35)$$

where

$$f_c(k; m) = 3.71 \cdot 10^{45} (3-k)^{\frac{(4-3k)m}{2(k-3)(1+m)}} (2+m)^2 10^{\frac{64.67+k(16.17k-2.59m-70.06)+3.45m}{(k-3)(1+m)}}; \quad (36)$$

$$a = f_a(k; m) (1+X)^{3=5} (1+Y) (1+z)^{\frac{9k+m-13}{5(1+m)}} A^{\frac{9k-13m-27}{5(k-3)(1+m)}} E_0^{\frac{(9k-14)m}{5(k-3)(1+m)}} E_0^{\frac{2(9k-14)(k+m-3)}{5(k-3)(1+m)}} \quad (37)$$

$$\frac{6=5}{B} t_e^{\frac{9k+6m-8}{5(1+m)}} H z;$$

where

$$f_a(k; m) = 4.05 \cdot 10^{19} (3-k)^{\frac{(9k-14)m}{5(k-3)(1+m)}} (2+m)^{-1} 10^{\frac{k(75.44-19.40k-9.83m)+33.96m-51.73}{(k-3)(1+m)}}; \quad (38)$$

$$F_m = f_F(k; m) p A^{\frac{3k-m-9}{2(k-3)(1+m)}} (1+X) (1+z)^{\frac{3k+4m-4}{2(1+m)}} E_0^{\frac{(3k-8)m}{2(k-3)(1+m)}} E_0^{\frac{(3k-8)(k+m-3)}{(k-3)(1+m)}} \frac{1=2}{B} \quad (39)$$

$$d_1^2 t_e^{\frac{3k+2m-6}{2(1+m)}} \text{ergs}^{-1} \text{cm}^{-2};$$

where

$$f_F(k; m) = 2.42 \cdot 10^{-21} [53.32 (3 - k)]^{\frac{6+k(m-2)-2m}{2(k-3)(1+m)}} 10^{\frac{32.33-16.17k-10.78m}{1+m}} : \quad (40)$$

The time when $t_m = t_c$ is given by

$$t_{cm} = f_{cm}(k; m) \frac{(1+Y)(p-2)^{\frac{1+m}{k+m-1}}}{(1+X)(p-1)} (1+z) x_p^{\frac{1+m}{2(k+m-1)}} A^{\frac{k-m-3}{(k-3)(k+m-1)}} E_0^{\frac{(k-2)m}{(k-3)(k+m-1)}} E_0^{\frac{2(k-2)(k+m-3)}{(k-3)(k+m-1)}} (B_e)^{\frac{1+m}{k+m-1}} ; \quad (41)$$

where

$$f_{cm}(k; m) = 1.67 \cdot 10^{-11} \frac{8.82 \cdot 10^{-17} \frac{1+m}{k+m-1}}{2+m} [53.32 (3 - k)]^{\frac{(k-2)m}{(k-3)(k+m-1)}} : \quad (42)$$

for the case of an adiabatic break ($t_{cm} < t_{jet}$), and by

$$t_{cm}^r = f_{cm}^r(m) \frac{(1+Y)(p-2)}{(1+X)(p-1)} (1+z) x_p^{1=2} A^{1=3} E_0^{2=3} E_0^{\frac{4}{3} + \frac{4}{m}} B_e^{4=m} s; \quad (43)$$

where

$$f_{cm}^r(m) = 1.47 \cdot 10^{-27} \frac{(4.91 \cdot 10^{-10})^{\frac{1}{1+m}}}{2+m} 10^{\frac{10.78+1.47m}{1+m}} : \quad (44)$$

for the case of a radiative break ($t_{jet}^a < t_{cm}$). The break time when a relativistic jet begins to spread exponentially is given by

$$t_{jet} = f_{jet}(k; m) (1+z) A^{\frac{1}{k-3}} E_0^{\frac{1}{k-3}} E_0^{2(\frac{1}{k-3} + \frac{1}{m})} E_0^{2+\frac{2}{m}} s; \quad (45)$$

where

$$f_{jet}(k; m) = (5.22 \cdot 10^{-24})^{\frac{1}{k-3}} (6.00 \cdot 10^{-10})^{\frac{5-k}{k-3}} (3 - k)^{\frac{1}{k-3}} : \quad (46)$$

for the case of a radiative break, and by

$$t_{jet}^a = f_{jet}^a(k; m) \frac{(1+Y)(p-2)^{\frac{m-3}{3(m-1)}}}{(1+X)(p-1)} (1+z)^{\frac{3-m}{3(1+m)}} x_p^{\frac{m-3}{6(m-1)}} A^{\frac{5m-9}{9(m-1)}} E_0^{\frac{2m}{9(m-1)}} E_0^{\frac{4(m-3)}{9(m-1)}} (B_e)^{\frac{m-3}{3(m-1)}} E_0^{8=3} s; \quad (47)$$

where

$$f_{jet}^a(k; m) = 4.17 \cdot 10^{-12} 159.96^{\frac{2m}{9(m-1)}} \frac{8.82 \cdot 10^{-17} \frac{m-3}{3(m-1)}}{2+m} (1+m) : \quad (48)$$

for the case of an adiabatic break.

REFERENCES

Berger, E. et al. 2000, ApJ, 545, 56

Berger, E. et al. 2001, ApJ, 556, 556

- Blandford, R. D. & McKee, C. F. 1976, *Phys. Fluids*, 19, 1130
- Bottcher, M. & Demer, C. D. 2000, *ApJ*, 532, 281
- Castro-Tirado, A. J. et al. 1999, *Science*, 283, 2069
- Chiang, J. & Demer, C. D. 1999, *ApJ*, 512, 699.
- Cohen, E., Piran, T. & Sari, R. 1998, *ApJ*, 509, 717
- Covino, S. et al. 1999, *A & A*, 348, L1
- Cowsik, R. et al. 2001, *BASI*, in press (astro-ph/0104363)
- Dai, Z. G. & Cheng, K. S. 2001, *ApJ*, 558, L109
- Dai, Z. G., Huang, Y. F. & Lu, T. 2001, *MNRAS*, 324, L11
- Dai, Z. G. & Lu, T. 1999, *ApJ*, 519, L155
- Dai, Z. G. & Lu, T. 2000, *ApJ*, 537, 803
- Demer, C. D., Bottcher, M. & Chiang, J. 2000, *ApJ*, 537, 255
- Fruchter, A. S. et al. 1999, *ApJ*, 519, L13
- Galam, T. J. et al. 1999, *Nature*, 398, 394
- Galam, T. J. & Wijers, R. A. M. J. 2001, *ApJ*, 549, L209
- Gou, L. J., Dai, Z. G., Huang, Y. F. & Lu, T. 2001, *A & A*, 368, 464
- Granot, J., Piran, T. & Sari, R. 1999, *ApJ*, 527, 236
- Halpern, J. P. et al. 2000, *ApJ*, 543, 697
- Harrison, F. A. et al. 1999, *ApJ*, 523, L121
- Harrison, F. A. et al. 2001, *ApJ*, 559, 123
- Huang, Y. F., Dai, Z. G. & Lu, T. 2000b, *MNRAS*, 316, 943
- Huang, Y. F., Gou, L. J., Dai, Z. G. & Lu, T. 2000a, *ApJ*, 543, 90
- in 't Zand, J. J. M. et al. 2001, *ApJ*, 559, 710
- Jensen, B. L. et al. 2001, *A & A*, 370, 909
- Kulkarni, S. R. et al. 1999, *Nature*, 398, 389
- Masetti, N. et al. 2000, *A & A*, 359, L23
- Masetti, N. et al. 2001, *A & A*, 374, 382
- Meszáros, P. & Rees, M. J. 1997, *ApJ*, 476, 232
- Meszáros, P., Rees, M. J. & Wijers, R. A. M. J. 1997, *ApJ*, 499, 301
- Moder, R., Sikora, M. & Bulik, T. 2000, *ApJ*, 529, 151
- Paczynski, B. & Rhoads, J. 1993, *ApJ*, 418, L5
- Paczynski, B. & Xu, G., 1994, *ApJ*, 424, 708
- Panaitescu, A. & Meszáros, P. 1998, *ApJ*, 501, 772
- Panaitescu, A. & Kumar, P. 2000, *ApJ*, 543, 66
- Panaitescu, A. 2001, *ApJ*, 556, 1002
- Piran, T. 1999, *Physics Reports*, 314, 575
- Piro, L. et al. 2001, *ApJ*, 558, 442
- Price, P. A. et al. 2001, *ApJ*, 549, L7
- Rees, M. J. & Meszáros, P. 1994, *ApJ*, 430, L93
- Rhoads, J. 1999, *ApJ*, 525, 737
- Rhoads, J. & Fruchter, A. S. 2001, *ApJ*, 546, 117
- Rybicki, G. B. & Lightman, A. P. 1979, *Radiative Processes in Astrophysics* (New York: Wiley Interscience), P. 189
- Sagar, R. et al. 2000, *BASI*, 28, 499
- Sagar, R. et al. 2001a, *BASI*, 29, 1

- Sagar, R. et al. 2001b, *BASI*, 29, 91
- Sari, R. & Esin, A. A. 2001, *ApJ*, 548, 787
- Sari, R., Piran, T. & Halpern, J. 1999, *ApJ*, 524, L43
- Sari, R., Piran, T. & Narayan, R. 1998, *ApJ*, 497, L17
- Stanek, K. Z. et al. 1999, *ApJ*, 522, L39
- Stanek, K. Z. et al. 2001, *ApJ*, in press (astro-ph/0104329)
- Totani, T. 1998, *ApJ*, 502, L13
- Vietri, M. 1997, *ApJ*, 478, L9
- van Paradijs, J., Kouveliotou, C., & Wijers, R. A. M. J. 2000, *A&A*, 38, 379
- Waxman, E. 1997a, *ApJ*, 485, L9
- Waxman, E. 1997b, *ApJ*, 489, L33
- Wei, D. M. & Lu, T. 1998, *ApJ*, 505, 252
- Wei, D. M. & Lu, T. 2000, *ApJ*, 541, 203
- Wijers, R. A. M. J. et al. 1999, *ApJ*, 523, L33
- Wijers, R. A. M. J. & Galama, T. J. 1999, *ApJ*, 523, 177
- Wijers, R. A. M. J., Rees, M. J., & Meszaros, P. 1997, *MNRAS*, 288, L51
- Zhang, B. & Meszaros, P. 2001, *ApJ*, 559, 110

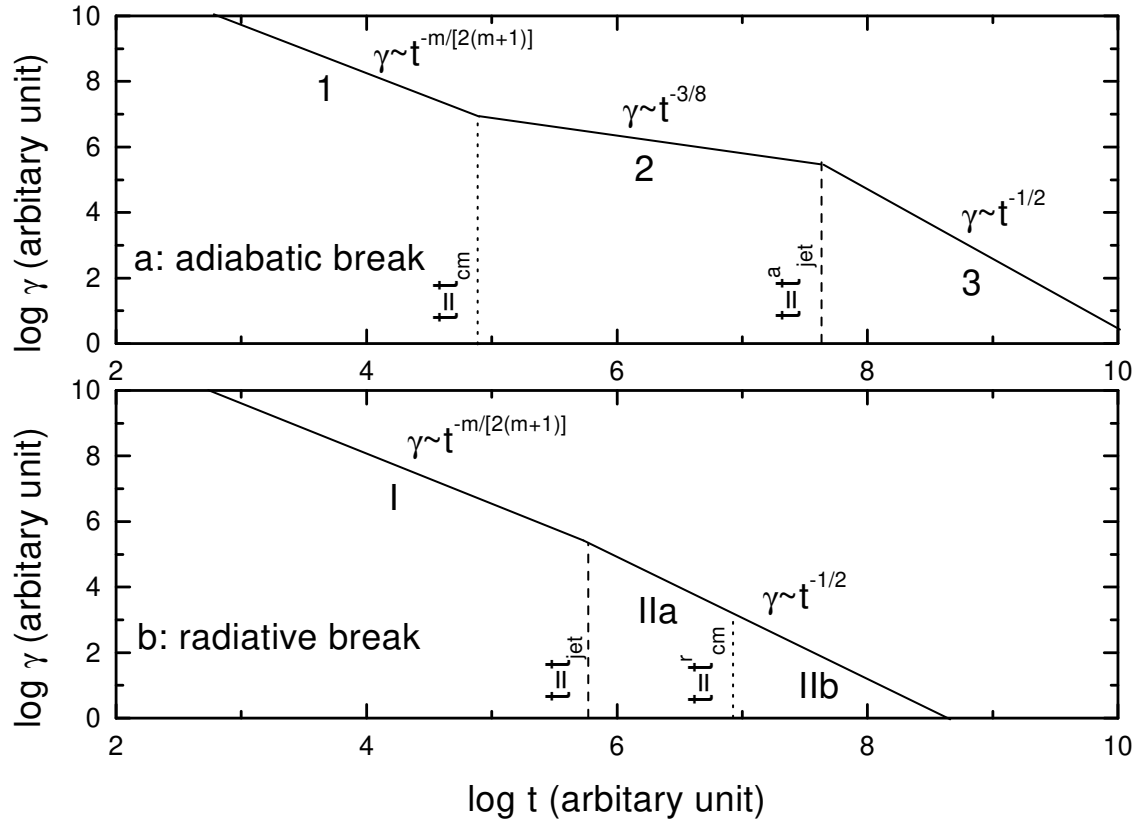


Figure 1. The Lorentz factor of a relativistic jet as a function of the observer's time (schematic). In the case of an adiabatic jet break (frame a), the relativistic jet evolves sequentially into (1) a radiative and spherical-like phase, (2) an adiabatic and spherical-like phase and (3) a spreading phase. In the case of a radiative jet break (frame b), the sequence becomes (I) a radiative and spherical-like phase and (II) a spreading phase which consists of two stages with fast-cooling (IIa) and slow-cooling (IIb) electrons, respectively. The times separating different phases are illustrated in the text.

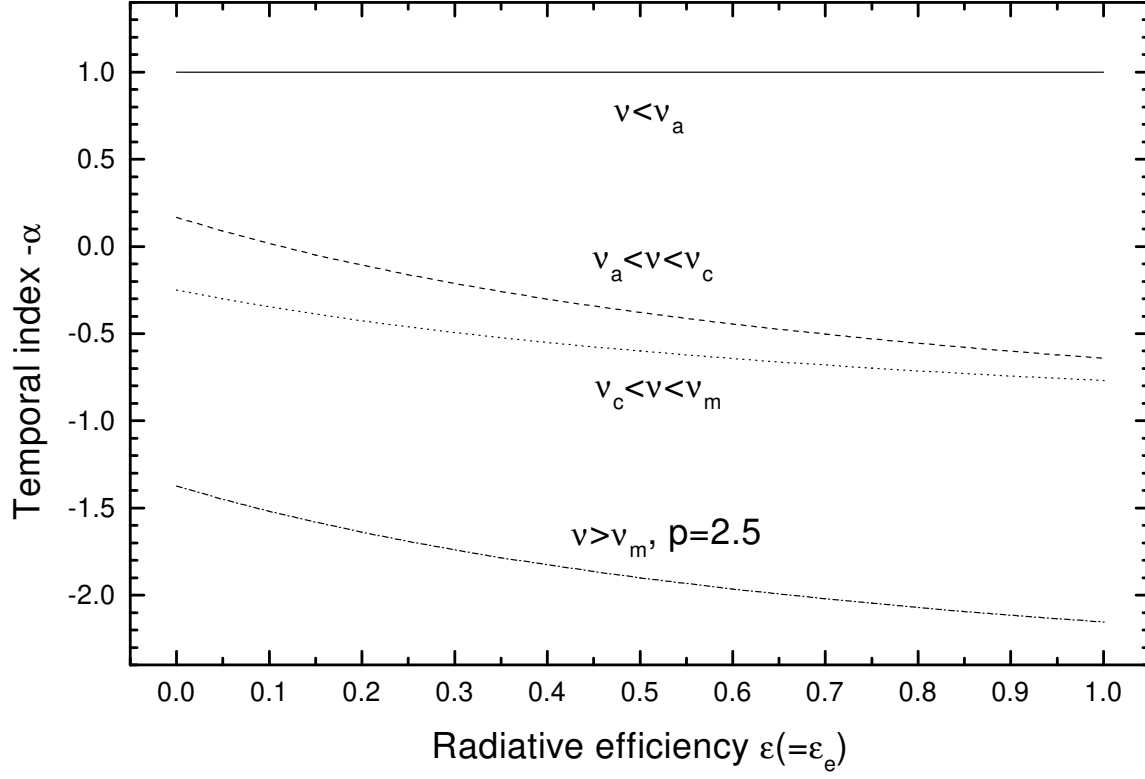


Figure 2. The relation between the light curve decay index and the radiative efficiency ($=\varepsilon_e$) in different energy bands for the spherical-like and radiative phase.

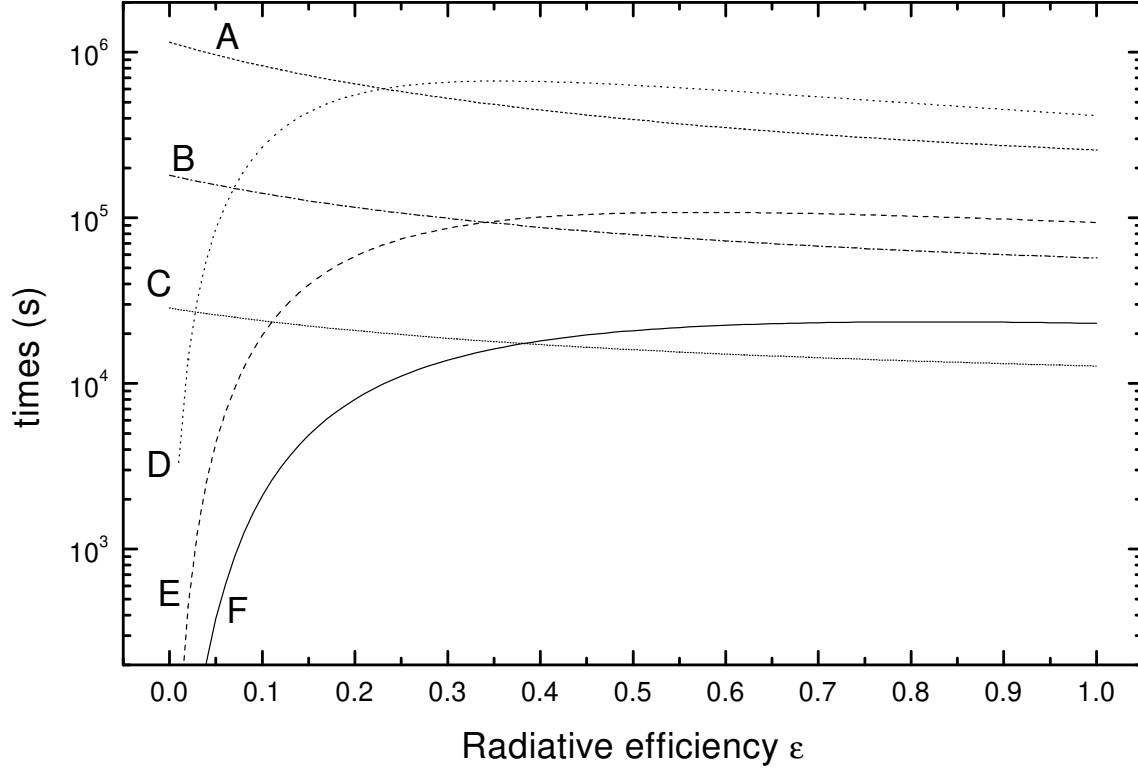


Figure 3. The times t_{cm} and t_{jet} as functions of radiative efficiency ($\epsilon = \epsilon_e$) with different parameters: curves A, B and C show the time t_{jet} with $\epsilon_0 = 0.2, 0.1$ and 0.05 , respectively; curves D, E and F show the time t_{cm} with $\epsilon_B = 10^{-1}, 10^{-2}$ and 10^{-3} , respectively. The remaining parameters are set as $k = 0, X = 1, z = 1, A = 1 \text{ cm}^{-3}, p = 2.5, E_0 = 10^{53} \text{ erg}$, and $\epsilon_0 = 100$.

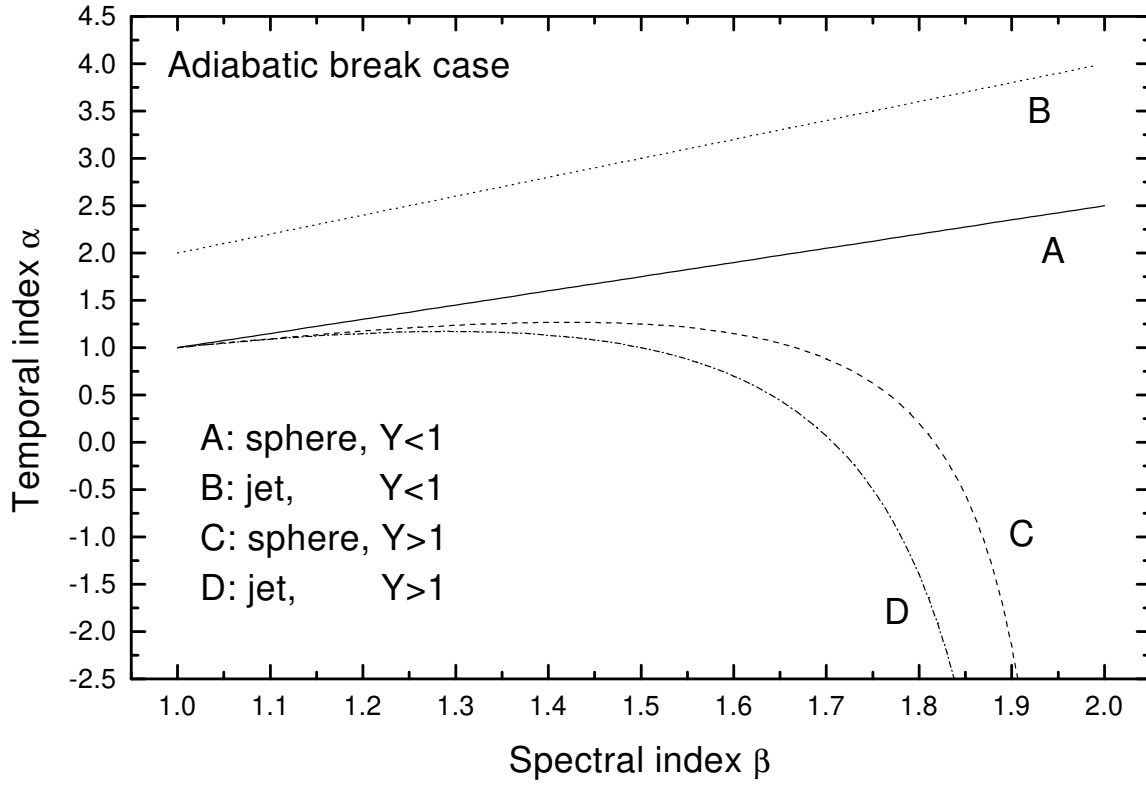


Figure 4. The relation between the light curve index α and the spectral index β above β_c in the case of an adiabatic jet break. The cases A and C correspond to times before the jet break, while B and D correspond to times after the jet break.

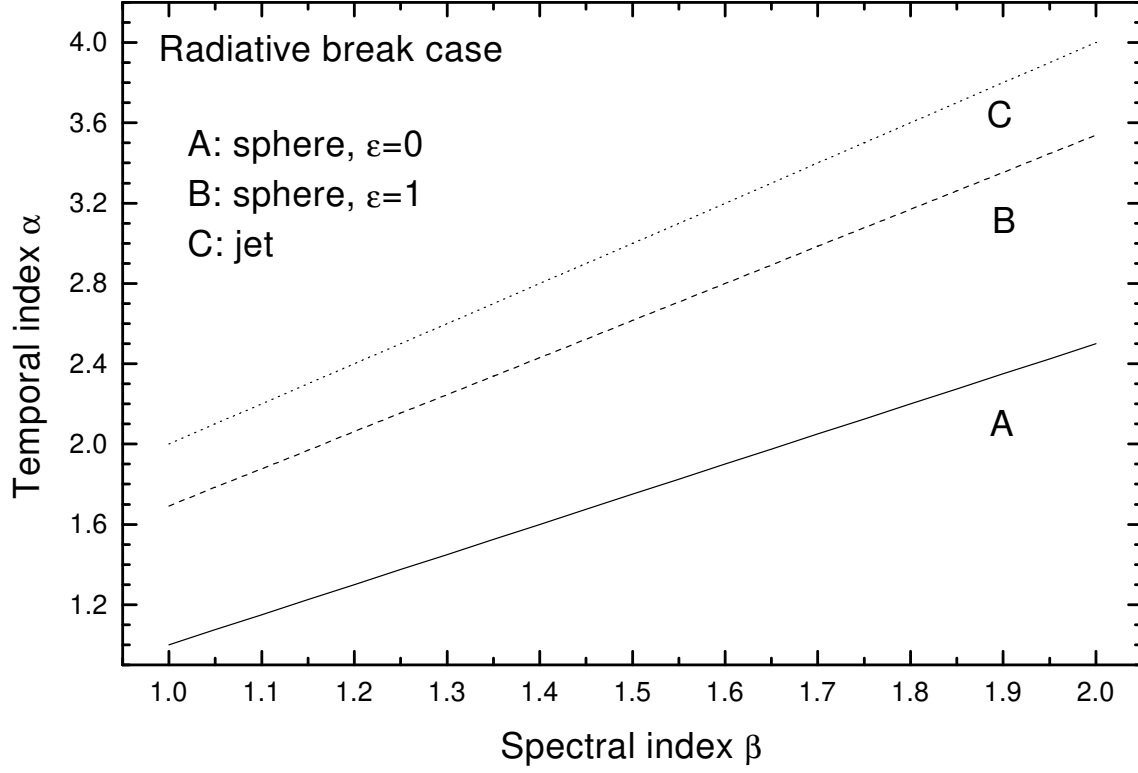


Figure 5. Same as Fig. 4 but at the energy band above ν_m in the case of a radiative jet break. Curves A and B correspond to the spherical-like phase with $\varepsilon = 0$ and 1, respectively. The cases for $0 < \varepsilon < 1$ are located in the regime between A and B. Curve C corresponds to the spreading phase.